

Surface inspection by monitoring spectral shifts of localized plasmon resonances

P. Albella*, F. Moreno, J. M. Saiz, and F. González

Grupo de Óptica, Departamento de Física Aplicada, Universidad de Cantabria

Avda. De los Castros SN, 39005 Santander, Spain

*Corresponding author: albellap@unican.es

Abstract: We present a numerical study of the spectral variations of localized surface plasmon resonances (LSPR) in a 3D-probe metallic nanoparticle scanned over an inhomogeneous dielectric surface. The possibilities for both, index monitoring and lateral resolution at nanoscale level are explored, with special attention paid to the shape of the probe and the profile of the near field underneath.

©2008 Optical Society of America

OCIS codes: (000.0000) General. [180.0180](#), [300.0300](#)

References and links

1. H. Raether, *Surface Plasmons on Smooth and Rough Surfaces and on Gratings* (Springer-Verlag, Berlin, 1988).
2. R. A. Jensen, J. Sherin and S. R. Emory. "Single Nanoparticle Based Optical pH Probe," *Appl. Spectr.* **61**, 832-838 (2007).
3. W. R. Holland and D. G. Hall. "Surface-plasmon dispersion relation: Shifts induced by the interaction with localized plasma resonances," *Phys. Rev.* **B 27**, 7765-7768 (1983).
4. T. Wang and W. Lin. "Electro-optically modulated localized surface plasmon resonance biosensors with gold nanoparticles," *Appl. Phys. Lett.* **89**, 173903 (2006).
5. A. D. McFarland and R. P. Van Duyne. "Single Silver Nanoparticles as Real-Time Optical Sensors with Zeptomole Sensitivity," *Nano. Lett.* **3**, 1057-1062 (2003).
6. A. Haes and R. P. Van Duyne. "A Nanoscale Optical Biosensor: Sensitivity and Selectivity of an Approach Based on the Localized Surface Plasmon Resonance Spectroscopy of Triangular Silver Nanoparticles," *J. Am. Chem. Soc.* **124**, 10596-10604 (2002).
7. T. Kalkbrenner, U. Håkanson and V. Sandoghdar. "Tomographic Plasmon Spectroscopy of a Single Gold Nanoparticle," *Nano. Lett.* **4**, 2309-2314 (2004).
8. T. Kalkbrenner, U. Håkanson, A. Schädle, S. Burger, C. Henkel and V. Sandoghdar. "Optical Microscopy via Spectral Modifications of a Nanoantenna," *PRL* **95**, 200801 (2005).
9. F. Moreno, F. González, and J. M. Saiz. "Plasmon spectroscopy of metallic nanoparticles above flat dielectric substrates," *Opt. Lett.* **31**, 1902-1904 (2006).
10. A.L. González and C. Noguez. "Influence of Morphology on the Optical Properties of Metal Nanoparticles," *J. of Computational and Theoretical Nanoscience* **4**, 231-238 (2007).
11. G.C. Schatz. "Electrodynamics of nonspherical noble metal nanoparticles and nanoparticle aggregates," *J. Mol. Struct. (Theochem.)* **573**, 73-80 (2001).
12. E.M. Purcell, C.R. Pennypacker. "Scattering and absorption of light by non-spherical dielectric grains," *J. Astrophys.* **186**, 705-714 (1973).
13. B. T. Draine and P. J. Flatau. "User Guide for the Discrete Dipole Approximation Code DDSCAT 6.1," <http://arxiv.org/abs/astro-ph/0409262v2>, (2004).
14. G. Lévêque and O. J. F. Martin. "Optical interactions in a plasmonic particle coupled to a metallic film," *Opt. Express.* **14**, 9971-9981 (2006).
15. E. D. Palik. *Handbook of Optical Constants of Solids*, (Academic Press, New York, 1985).
16. L. J. Sherry, R. Jin, C. A. Mirkin, G. C. Schatz and R. P. Van Duyne. "Localized Surface Plasmon Resonance Spectroscopy of Single Triangular Nanoprisms," *Nano. Lett.* **6**, 2060-2065 (2006).
17. L. J. Sherry, S. Chang, B.J. Wiley, Y. Xia, G. C. Schatz, and R. P. Van Duyne. "Localized Surface Plasmon Resonance Spectroscopy of Single Silver Nanocubes," *Nano. Lett.* **5**, 2034-2038 (2005).

18. J. J. Mock, D. R. Smith and S. Schultz. "Local refractive index dependence of plasmon resonance spectra from individual nanoparticles," *Nano Lett.* **3**, 485-491 (2003).
 19. C. Noguez. "Optical properties of isolated and supported metal nanoparticles," *Opt. Mater.* **27**, 1204-1211 (2005).
-

1. Introduction

Metallic nanoparticles (MNPs) made of silver or gold show exceptional optical properties when illuminated with visible light at the appropriate wavelength. Resonances can be excited due to the collective oscillation of the quasi-free plasma electrons present in metals. These resonances, known as Localized Plasmon Resonances or Localized Surface Plasmons resonances (LSPR), because the collective excitation is often located very close to the surface, produce a high scattering cross section and intense electric field in the surroundings of the particles [1]. In addition, there is the possibility of tuning the resonances in the visible and near-infrared by changing the particle size and shape, the surrounding medium or both. All these properties make LSPR's suitable for the sensitive detection of changes in the MNPs local environments and therefore very useful for many interesting applications, such as molecular spectroscopy (SERS, molecular sensing), biomedicine (biosensors and biomarkers), telecommunications, fabrication and inspection of new optoelectronic devices, etc [2-6].

As stated before, the scattering cross-section of small particles depends strongly on their size, morphology and refractive index. In particular, silver NPs show pronounced resonances in the optical range. The study of such resonances, especially its position, can reveal information about the internal dynamics of the electronic motion and therefore about the possible changes in the optical properties of its surroundings[7,8].

The rational design of MNP-based sensors to optimize their performance parameter like the sensitivity, detection limit, resolution, and dynamic range for a specific application requires a systematic development of quantitative relationships between the composition, structure, and shape of different metal NPs and their optical properties. However, at the present time, only limited experimental information on these relationships is available, and we have to rely on simulations computationally intensive, to know about the optical response of MNPs attached to substrates. Whereas for a spherical particle placed in a homogeneous medium, the spectral cross section can be calculated straight forward using Mie theory based on a multipole expansion, when we deal with more complex structures, Mie theory cannot be applied and therefore we have to rely on more sophisticated computational methods like Extinction's Theorem, Discrete dipole approximation, Finite difference time domain, etc [9-11].

The objective of this work is to go deeper in the optical microscopy based on the study of the modifications suffered by the local fields produced in the surrounding of a metallic nanoparticle due to the presence of an inhomogeneous substrate. In particular, the configuration used in our numerical study is based on the experiments performed by T. Kalkbrenner et. al and published in refs. [7,8], where the authors analyze the surface topography of a sample by measuring the spectral changes suffered by a plasmon resonance (width and shift) excited in a gold nanoparticle, acting as a nanoantenna.

In this sense, we present a numerical simulation based on the discrete dipole approximation method (DDA), in which we monitor the changes in the optical response of a nanostructure by analyzing the changes in the spectral of the LSPR for a nanoscopic metallic tip scanned close to a dielectric sample. We first show the sensitivity of this monitoring to the presence of an inhomogeneity and then we study the spatial (lateral) resolution. Finally we will show from a near field point of view, how this scanning strongly depends on the shape of the tip and therefore it can be improved by using an adequate shape for the tip.

2. LSPR surface inspection

The most common method for LSPR sensing and microscopy (LSPRM) is the wavelength-shift measurement, in which the change in the maximum (or minimum) of the scattering curve associated to the LSPR is monitored as a function of the changes in the local surface depth and dielectric environment. A practical procedure for analyzing this technique is to scan a nanometric particle over the substrate and monitor the nanometric inhomogeneities that could be present in the substrate.

2.1 Scanning procedure

A nanometric particle, acting as a nanoantenna, is moved along the x axis of the sample and its plasmonic spectrum is calculated at each position of the tip. The system is illuminated at normal incidence with a plane wave polarized along the z -axis, as shown in Fig. 1. The sample consists of a square dielectric substrate of length L and height H which presents a nanometric region of index n' and width d , the inhomogeneity stripe, embedded in a material of index n . The origin of coordinates is taken on the substrate, in the middle of the inhomogeneity and x_t represents the distance of the center of the tip to this origin.

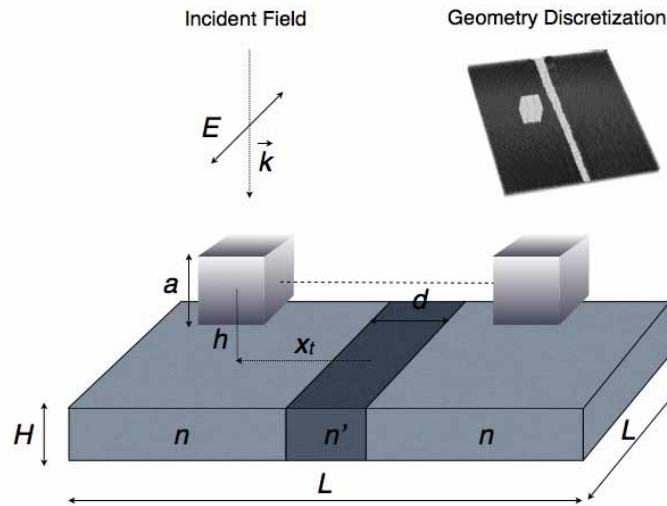


Fig. 1. Schematics of the geometry arrangement. Geometry discretization is shown in the inset. The length of the substrate L may vary from 180 nm to 200 nm , depending on the width d . The height of the substrate H has been fixed to 20 nm (similar height for the substrate is used by G.C. Schatz in ref. [11])

Backscattering cross section values are obtained for the spectral region around the LSPR of the material by using the Discrete dipole approximation (DDA) method which is a finite element-based approach for solving Maxwell equations [12,13]. The silver nanoparticle and substrate are modelled as rectangular hexahedrons (i.e. a cubic particle) made of silver, as this type of geometries have been probed very useful in the study of light scattering by nanoparticles over substrates [14].

All calculations refer to a silver probe whose optical constants are taken from the bulk material [15]. All the results that will be shown later have been compared to those from several earlier studies in which the DDA method has been calibrated by comparison with experiment for hexahedral particles [16]. These include studies of external dielectric effects and substrate effects and therefore it may be expected that this simulation will provide with an accurate qualitative description of such results. Our simulation results have also been

compared to others obtained by another calculation method, such as the Extinction's theorem or FDTD [10, 17].

3. Simulation results

3.1 Surface monitoring simulation

In Fig. 2 we present a simulation of the backscattering cross section obtained for 2 different situations: 1) Isolated and 2) with the presence of an inhomogeneous substrate, both are related to a nanoparticle of $a = 40$ nm and to an inhomogeneity of $d = 40$ nm and index $n' = 1.5$ embedded in a substrate of index $n = 1.4$. In the first situation, we only plot the dipolar resonance, which as expected for a cubic shaped silver nanoparticle of $a = 40$ nm, it is obtained at $\lambda = 410$ nm. In the second situation, when the substrate is present, we differentiate two different positions of the tip: one located at $x_t = -50$ nm, that is, the tip sees only the substrate with $n = 1.4$ and another with the tip located at $x_t = -10$ nm, where the tip sees the substrate of refractive index n and the inhomogeneity $n' = 1.5$. It can be seen that the presence of the substrate induces a shift of this dipolar resonance to longer wavelengths, and that this shift is strongly dependent on the optical properties of the substrate, obtaining higher red shifts as $\Delta n = n' - n$ increases. A secondary peak appears around 410 nm, due to the proximity of the tip to the substrate ($h \cong 2$ nm). This higher order resonance is caused by the strong substrate-particle interaction which excites higher order modes of charge oscillation. This general trend of the spectrum agrees very well with numerical and experimental results obtained by other authors [17-19], obtaining an approximate ratio between the red shift $\Delta\lambda_{LSPR}$ and the refractive index change of the substrate Δn of $\Delta\lambda_{LSPR} / \Delta n \cong 100$ nm, though it depends on the value of d .

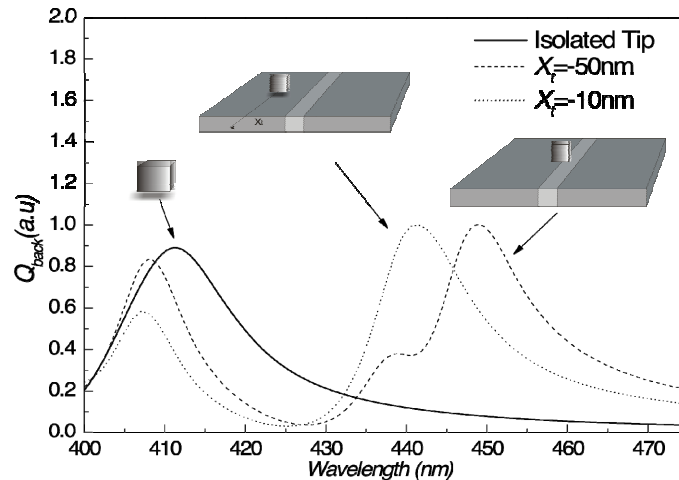


Fig. 2. Comparison of the Backscattering cross section calculated for an isolated cubic tip of side $a = 40$ nm (dotted line) and for the same tip scanned along the x axis of a substrate showing two particular positions: $x_t = -50$ nm (plain) and $x_t = -10$ nm (dashed).

In our study we use this dependence of the shift suffered by the LSPR to identify and characterize possible inhomogeneities.

3.2 Sensitivity to refractive index

In order to evaluate the sensitivity of this surface inspection method when used to detect and identify inhomogeneities in a substrate it is necessary to define a new parameter able to provide information about the substrate material the tip is “sensing” at each point of the surface. This parameter can be defined as $\Delta\lambda_{LSPR} = [\lambda]_{LSPR}(n') - [\lambda]_{LSPR}(n)$ and it represents

the LSPR shift induced by the inhomogeneity as related to a baseline shift corresponding to a substrate of index n that we take here as $n = 1.4$.

Figure 3 shows $\Delta\lambda_{LSPR}$ obtained for 3 different inhomogeneities, $n' = 1.42$, $n' = 1.46$ and $n' = 1.5$. According to previous qualitative results for $n' > n$ positive values of $\Delta\lambda_{LSPR}$ are expected for these cases and found in our calculations. It is interesting to notice how $\Delta\lambda_{LSPR}$ increases smoothly as the particle approaches the inhomogeneity. The maximum shift values reached in each situation are, respectively, $\Delta\lambda_{LSPR} = 2, 5$ and 8.5 nm for $\Delta n = 0.02, 0.06$ and 0.1 , showing an approximate linear dependence with Δn . Another interesting characteristic of $\Delta\lambda_{LSPR}$ is observed when the NP approaches $x_i = 0$, i.e., it is exactly centered on the inhomogeneity. Then $\Delta\lambda_{LSPR}$ presents a decay whose value depends on d , a , n' and also on the distance of the tip to the substrate, h . It is a kind of “shadow” produced by the tip at normal incidence. We will pay more attention to this effect in the following section.

It is worth mentioning that the scanning step and the wavelength sampling has been fixed to 2 nm and 1 nm, respectively. This would cause a discretization in the curves if the selection criterium for the maximum in the spectrum is simply the maximum among the calculated points. However, if we resort to a fit of the spectrum maxima, this describes a set of softer curves as the ones plotted in the following figures.

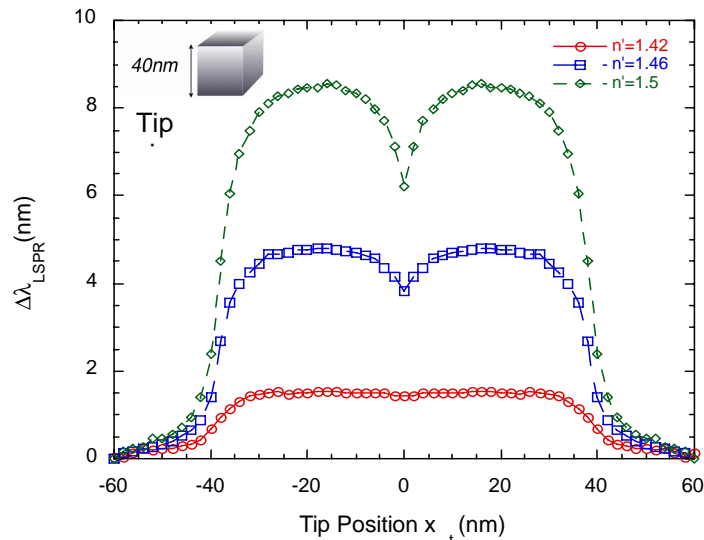


Fig. 3. Surface Plasmon shift ($\Delta\lambda_{LSPR}$) calculated for different values of n' . The substrate refractive index is fixed to $n = 1.4$. The tip size is shown in the inset.

3.3 Sensitivity to inhomogeneity size

Once we know that surface inspection by spectral shift monitoring of LSPR is sensitive to small changes in the refractive index we should establish whether it is possible to determine the size of this inhomogeneity and if so, the minimum width that could be detected. In Fig. 4 we show $\Delta\lambda_{LSPR}$ for 4 values of the size of the inhomogeneity, d : 20, 32, 40 and 60 nm, all of them with the same refractive index for the inhomogeneity: $n' = 1.5$. Again, we obtain similar profiles for the 3 widths except for 2 important differences: 1) the artifact around $x_t = 0$ decays as the width of the inhomogeneity increases, disappearing for values of $d > a$; and 2) the maximum value of $\Delta\lambda_{LSPR}$ saturates very fast to a limit as we increase the size of the inhomogeneity. This behaviour can be explained with the effective index theory, bearing in mind that in our case we can only talk about a pseudo effective refractive index, because the particle is not immersed in a n' refractive index. The effective index has to be weighed by the width of the inhomogeneity, gaining higher values for higher values of d .

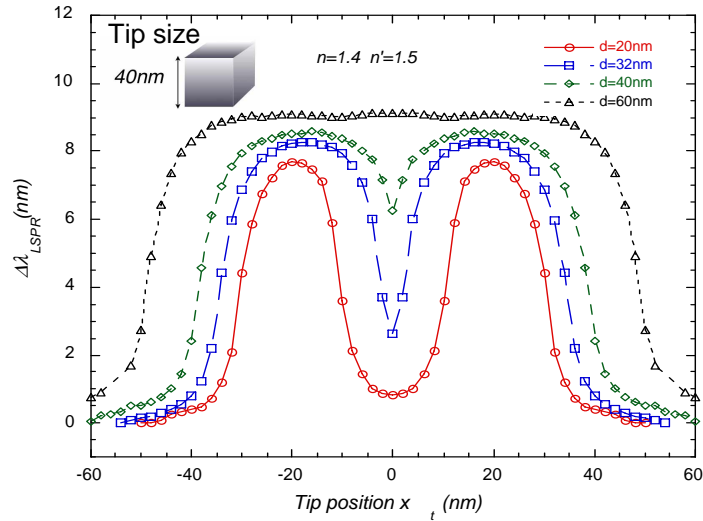


Fig. 4. Surface Plasmon shift ($\Delta\lambda_{LSPR}$) calculated for different values of d . The substrate and inhomogeneity refractive indexes are fixed to $n = 1.4$ and $n' = 1.5$ respectively.

Finally, this technique give rise to one question: is it possible to resolve 2 continuous inhomogeneities using this scanning procedure? The answer is *yes*, but under certain conditions. First, the distance between the 2 inhomogeneities must be at least 2 times the tip size, otherwise the two maxima obtained for each inhomogeneity would overlap. Second, Δn must be large enough to provide with a large enough value of the maximum and finally it will also depend on the size of the sensing nanoparticle. Figure 5 shows as an example 2 inhomogeneities of different refractive indexes, $n'=1.46$ and $n''=1.5$ embedded in a substrate of index $n = 1.4$. The length of this inhomogeneities is $d = 80$ nm and the separation between them is 80 nm.

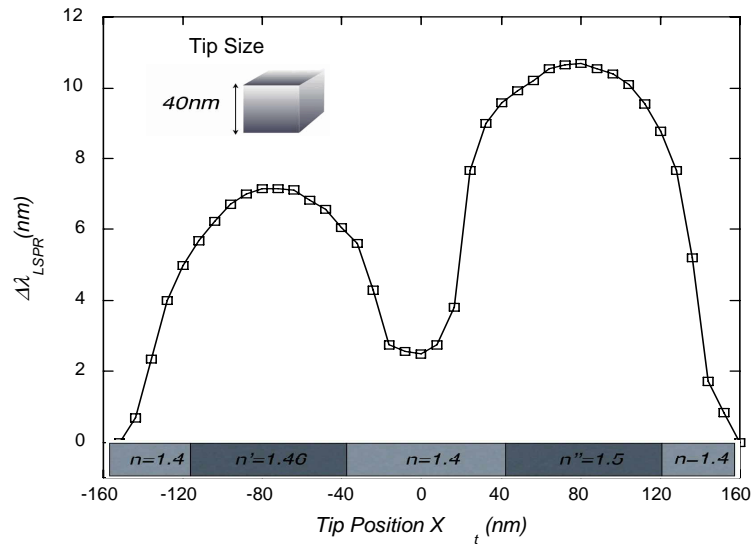


Fig. 5. Example of spatial resolution of 2 stripe inhomogeneities of $d=80$ nm and separated 80 nm.

3.4 Tip shape considerations (shadowing effect)

We have studied so far how sensitive this surface scanning method is to changes in the optical properties and to the size of some irregularity in the substrate underneath. We must consider now the shape of the tip itself, as it can be crucial when dealing with small inhomogeneities. In fact, from a practical point of view, rounded shapes can be more effective than planar shapes in the sense that their local field distribution appears less dispersed. In Figs. 6(a) and 6(b) we show a comparison of the near electric field obtained for two differently shaped tips, with square and circular profiles, both made of silver and of similar volumes. The near field shown in Figs. 6(a) and 6(b) has been obtained for incident wavelengths corresponding to their dipolar resonances, $\lambda_1 = 450 \text{ nm}$ and $\lambda_2 = 390 \text{ nm}$ respectively. We see how the near field reaches a certain distance at the sides of the particle, and also a minimum of the electric field under both particles. This explains how the tip starts to be sensitive before reaching the inhomogeneity, therefore establishing a value of approximately twice its size as a fundamental resolution limit. However, the central minimum has a special interest. First, it is the cause of the artifact, or central depression observed in Fig. 4. Second, it explains why it becomes more notorious when the size of the inhomogeneity is smaller than the nanoparticle. In this sense, the resolution limit would be reduced to the size of this “shadow”, smaller than the probe itself.

For an easier quantitative comparison, we show in Figs. 6(c) and 6(d) line plots at $h=1 \text{ nm}$ of the local electric field for each geometry, showing the great difference in the size of the “shadow”.

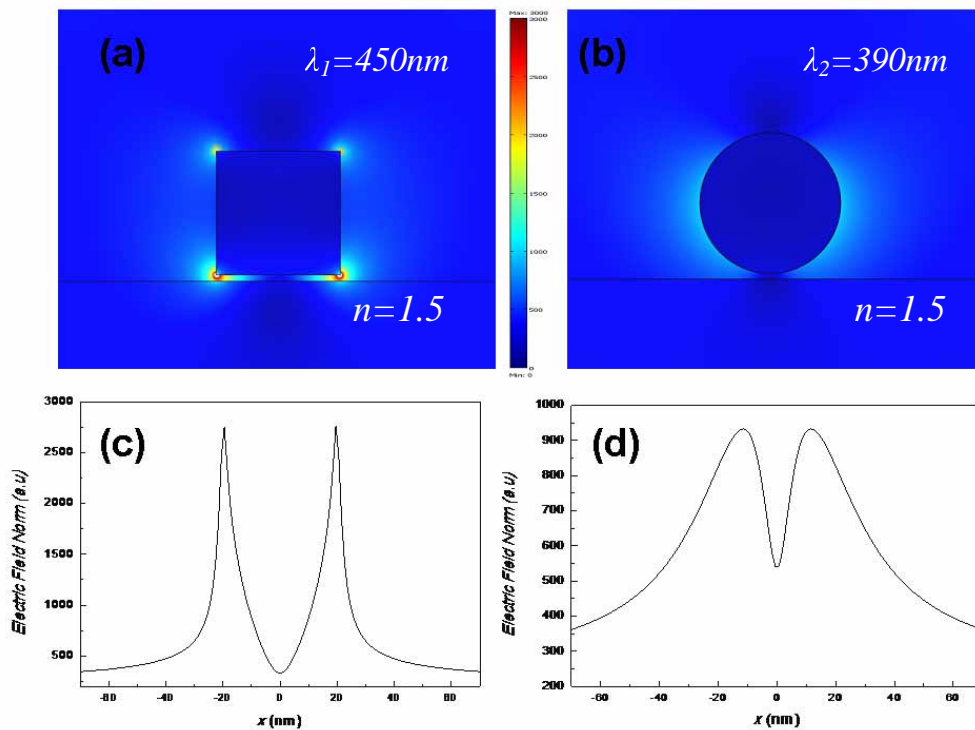


Fig. 6. (a). Near Field plot for a square profile tip of size $a = 40 \text{ nm}$ located at $h = 2 \text{ nm}$ height from a glass substrate. (b) Near Field plot for a circular profile tip of diameter $d = 50 \text{ nm}$ located at 1 nm height from a glass substrate. (c) and (d) line plots at $h=1 \text{ nm}$ of the local electric field for two different tips: square and circular, respectively.

4. Conclusions

In summary, we have seen along this paper how we can take advantage of the main consequence of exciting a LSPR on single nanoparticle: the generation of locally enhanced or amplified electromagnetic fields at the nanoparticle surface.

Because the material, size and shape, and also the dielectric environment dictate the characteristics of the LSPR, these properties can be taken in consideration for monitoring the possible changes in the surface of a nanostructured substrate. In particular, we have described numerically the light scattering by a metallic nanoparticle located on an inhomogeneous dielectric substrate and we have explored the possibilities of a scanning process of such nanoparticle acting as a probe tip, analyzing the plasmonic emission spectrum and the shift in its maximum. This maximum is very sensitive to the small variations in the refractive index. This configuration has been experimentally used before [7,8] for the topographic analysis of surface samples.

Moving the probe tip along the stripe inhomogeneity we observe that the shift in the maximum informs of the changes in the refractive index with an approximate resolution of twice the size of the tip, but with the particularity that small inhomogeneities induce “back steps” in the shift when the tip is centered on the inhomogeneity. This produces a depression in the shift monitoring appearing as an “artifact”.

The considerations we have made about the influence of the shape of the particle and the presence of a local depression of the electric field in the near field distribution close to the substrate, allow us to explain the origin of the mentioned “artifact”, and at the same time they suggest the possibility of having a resolution directly connected to the size of the field depression.

We have also shown the importance of the nanoparticle shape on both the spectral location of the LSPR and its sensitivity to changes in the local refractive index, showing that it is also necessary to model the tip if we want to make quantitative studies. In particular, we have shown how the “shadow” is far less pronounced in the case of rounded shaped tips when compared with squared shaped probes. This point can be crucial in applying our proposed scanning scheme to surface inspection when interpreting the signal. An interesting application of this study could be to define proper resolution criteria for different shapes of real probe tips.

Another variable that must be taken into account when applying this surface monitoring method is the distance of the tip to the substrate. The LSRP shifts are smaller as the distance tip-substrate increases. Moreover, if we want to obtain significant shifts for distances like the ones used in Ref. [8] by Kalkbrenner et. al (≈ 5 nm) we would have to increase the size of the resonant particle. In fact, in Ref. [8] the size of the particle used in their experiment is 100 nm.

Although, from a practical point of view, these parameters (shape and distance of the tip to the substrate) can be difficult to control, it is interesting to point out the high sensitivity of this scan to small changes in the inhomogeneity, such as size (d) and refractive index (Δn).

Acknowledgments

This research has been supported by the Ministry of Education of Spain under project #FIS2007-60158. The authors thankfully acknowledge the computer resources provided by the Spanish Supercomputing Network (RES) node at Universidad de Cantabria. P. Albella wants to express his gratitude to the Ministry of Education for his FPI grant.